Calculation of Electrochemical Reorganization Energies for Redox Molecules at Self–Assembled Monolayer Modified Electrodes

2 AUTHORS, INCLUDING:

Soumya Ghosh

University of Illinois, Urbana-Champaign

**9** PUBLICATIONS   **62** CITATIONS

Calculation of Electrochemical Reorganization Energies for Redox Molecules at Self-Assembled Monolayer Modified Electrodes

Soumya Ghosh and Sharon Hammes-Schiffer*

Department of Chemistry, University of Illinois at Urbana−Champaign, 600 South Mathews Avenue, Urbana, Illinois 61801, United States

S *Supporting Information*

ABSTRACT: Electrochemical electron transfer reactions play an important role in energy conversion processes with many technological applications. Electrodes modified by self-assembled monolayers (SAMs) exhibit reduced double layer effects and are used in molecular electronics. An important quantity for calculating the electron transfer rate constant is the reorganization energy, which is associated with changes in the solute geometry and the environment. In this Letter, an approach for calculating the electrochemical reorganization energy for a redox molecule attached to or near a SAM modified electrode is presented. This integral equations formalism polarizable continuum model (IEF-PCM) approach accounts for the detailed electronic structure of the molecule, as well as the contributions from the electrode, SAM, and electronic and inertial solvent responses. The calculated total reorganization energies are in good agreement with experimental data for a series of metal complexes in aqueous solution. This approach will be useful for calculating electron transfer rate constants for molecular electrocatalysts.
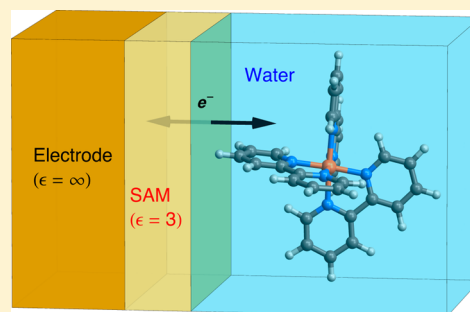
Self-assembled monolayer (SAM) modified electrodes have been used to study properties related to long-range electron transfer between redox-active molecules and electrodes. Properties of interest include reorganization energies and the distance dependence of metal-molecule electronic coupling.[1−6] Redox molecules that are directly attached to the SAMs have also been used in several chemical applications, such as anion sensing.[7] Additional applications of SAM modified electrodes include molecular electronics[8] and biofuel cells.[9] According to Marcus theory for electron transfer,[10] the electron transfer rate constant depends exponentially on the free energy barrier, which in turn depends on the reorganization energy.[11] The advantages of modifying the electrode with a SAM for reorganization energy measurements are that the double layer effects at the interface between electrode and the solvent are diminished,[12] and the distance between the molecule and the electrode can be determined more reliably. In this Letter, we present a quantum chemical method for calculating the electrochemical reorganization energy for redox molecules near SAM modified electrodes. We apply this approach to a series of redox molecules close to or covalently attached to the SAM, as depicted schematically in Figure 1, and compare the calculated values with experimental results.

The total electrochemical reorganization energy can be expressed as the sum of the inner-sphere and outer-sphere reorganization energies, which are associated with changes in the solute geometry and the environment, respectively, upon electron transfer. For a SAM modified electrode, the environment includes the solvent, SAM, and electrode; according to convention, the outer-sphere reorganization energy is still
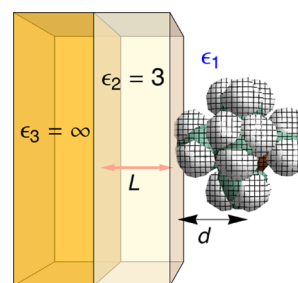

Figure 1. Schematic representation of a molecule near a SAM modified electrode. L and d represent the width of the SAM and the distance between the center of mass of the molecule and the SAM−solvent interface, respectively. The tesserae on the molecular cavity are depicted schematically.

denoted the solvent reorganization energy in this case. Typically the inner-sphere and outer-sphere reorganization energies are assumed to be uncoupled. Various methods have been developed for the calculation of the inner-sphere reorganization energy.[13−16] In the four-point method,[14] which is employed in the present study, the reduced and oxidized states of the molecule are optimized in the gas phase, and the energies of the oxidized and reduced species are calculated at each geometry and combined to generate the inner-sphere reorganization energy. This Letter focuses on the development of new methodology for calculating the solvent reorganization
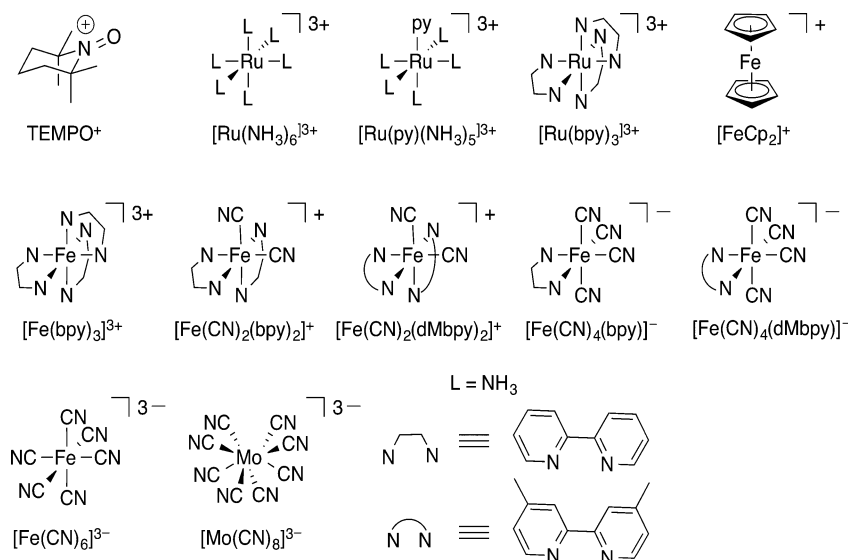
Figure 2. Series of molecules studied with the methods presented herein.

energies, which are added to the inner-sphere reorganization energies to produce the total reorganization energies for comparison to experimental results.

We have developed a method for calculating the electrochemical solvent reorganization energy for a SAM modified electrode within the framework of the Integral Equation Formalism Polarizable Continuum Model (IEF-PCM).[17−21] This method is an extension of our previous approach for calculating the electrochemical solvent reorganization energy without a SAM.[22] The solute geometry remains fixed during the calculation of the solvent reorganization energy, and the solvent response is separated into fast (predominantly electronic) and slow (inertial) components.[23−26] The solvent reorganization energy is calculated as the difference between a nonequilibrium and equilibrium free energy for either the reduced or the oxidized solute molecule, where the terms nonequilibrium and equilibrium refer to the inertial component of the solvent polarization. For the reduced (oxidized) molecule, the nonequilibrium inertial solvent polarization is associated with the equilibrium inertial solvent polarization for the oxidized (reduced) molecule. The electronic component of the solvent polarization is evaluated self-consistently with the solute charge density, denoted the self-consistent (SC) limit, using an algorithm reported elsewhere.[22] The total outer-sphere reorganization energy is the average of the outer-sphere reorganization energies calculated for reduction and oxidation of a redox molecule at the electrode.

Within the IEF-PCM framework, the molecule-solvent boundary is treated explicitly, and the effects of the other boundaries are included through an external Green's function. This approach accounts for the detailed electronic structure of the molecule, as well as the electrostatic contributions from the environment. In our previous implementation, the Green's function incorporated the effects of the electrode−solvent boundary. In the present work, we devise a form of the Green's function that incorporates both the electrode−SAM and the SAM−solvent boundary, as depicted in Figure 1. The electrode is modeled as a perfect conductor with a dielectric constant of $\varepsilon = \infty$, and the solvent is modeled as water with static and optical dielectric constants of $\varepsilon_0 = 78.39$ and $\varepsilon_\infty = 1.776$, respectively. The SAM is modeled as a region of low dielectric constant with

$\varepsilon = 3$, as determined from previous experiments.[27] We also tested the sensitivity of the outer-sphere reorganization energy to the SAM dielectric constant by performing calculations with the SAM dielectric constant chosen to be $\varepsilon = 5$. As shown in Supporting Information Table S1, the solvent reorganization energies decreased by ∼0.1 eV upon increasing the SAM dielectric constant from 3 to 5.

In our derivation, the Green's function equation for the Laplace operator was solved with the appropriate boundary conditions in cylindrical coordinates,[28] and the solution was subsequently transformed into Cartesian coordinates. The final form of the external Green's function is given by

$$G^E(\mathbf{r}, \mathbf{r}') = \frac{1}{\varepsilon_1}\left(\frac{1}{|\mathbf{r} - \mathbf{r}'|} - \eta_{2,1}\frac{1}{|\mathbf{r} - \mathbf{M}^{SAM}(\mathbf{r}')|} \right.$$
$$\left. + \frac{4\varepsilon_1\varepsilon_2}{(\varepsilon_1 + \varepsilon_2)^2} \sum_{m=1}^{\infty} (\eta_{2,1})^{m-1}(-1)^m \frac{1}{|\mathbf{r} - \mathbf{M}_m^{el}(\mathbf{r}')|} \right)$$

(1)

Here, $\mathbf{M}_m^{el}(\mathbf{r}')$ is the mth mirror image of the vector $\mathbf{r}'$ with respect to the electrode-SAM interface, $\mathbf{M}^{SAM}(\mathbf{r}')$ is the mirror image of the vector $\mathbf{r}'$ with respect to the SAM-solvent interface, $\eta_{2,1} = ((\varepsilon_2 - \varepsilon_1)/(\varepsilon_2 + \varepsilon_1))$, and ε_1 and ε_2 are the dielectric constants of water and the SAM, respectively. If the coordinate $\mathbf{r}'$ is given by (x', y', z'), $\mathbf{M}_m^{el}(\mathbf{r}')$ is given by $(x', y', 2d + 2mL - z')$ and $\mathbf{M}^{SAM}(\mathbf{r}')$ is given by $(x', y', 2d - z')$, where L and d are defined in Figure 1. As discussed in ref 22, separate calculations must be performed with the optical and static dielectric constants of water to obtain the outer-sphere reorganization energy; as in previous work,[28] the optical and static dielectric constants of the SAM are assumed to be the same.

In the PCM, the electrostatic effects of the environment are expressed in terms of an apparent surface charge density represented by a discrete set of point charges at the centers of discretized surface elements, denoted tesserae, on the surface of the molecular cavity. In the matrix-inversion formulation of the IEF-PCM, the surface charge density is determined by the solution of a matrix equation[22] that depends on the electrostatic potential at the center of each tessera induced by the solute charge density, as well as matrices related to the Green's

2

dx.doi.org/10.1021/jz5023784 | J. Phys. Chem. Lett. 2015, 6, 1−5

functions and their normal derivatives inside and outside of the cavity. The matrix elements of the $\mathbf{S}^E$ and $\mathbf{D}^E$ matrices, which are related to the Green's function and its normal derivative, respectively, outside of the cavity are

$$S_{ij}^E = \frac{1}{\varepsilon_1}\left[S_{ij}^I - \frac{a_i a_j}{4\pi}\left(\frac{\eta_{2,1}}{|\mathbf{r}_i - \mathbf{M}^{SAM}(\mathbf{r}_j)|}\right.\right.$$
$$\left.\left. - \frac{4\varepsilon_1\varepsilon_2}{(\varepsilon_2 + \varepsilon_1)^2}\sum_{m=1}^{\infty}(\eta_{2,1})^{m-1}(-1)^m\frac{1}{|\mathbf{r}_i - \mathbf{M}_m^{el}(\mathbf{r}_j)|}\right)\right] \tag{2}$$

$$D_{ij}^E = D_{ij}^I - \frac{a_i a_j}{4\pi}\left(\eta_{2,1}\frac{[\mathbf{r}_i - \mathbf{M}^{SAM}(\mathbf{r}_j)]\cdot\mathbf{n}_j}{|\mathbf{r}_i - \mathbf{M}^{SAM}(\mathbf{r}_j)|^3}\right.$$
$$\left. - \frac{4\varepsilon_1\varepsilon_2}{(\varepsilon_2 + \varepsilon_1)^2}\sum_{m=1}^{\infty}(\eta_{2,1})^{m-1}(-1)^m\frac{[\mathbf{r}_i - \mathbf{M}_m^{el}(\mathbf{r}_j)]\cdot\mathbf{n}_j}{|\mathbf{r}_i - \mathbf{M}_m^{el}(\mathbf{r}_j)|^3}\right) \tag{3}$$

where a_i is the area of the ith tessera and $\mathbf{n}_i$ is the unit vector normal to the surface of the ith tessera. Expressions for the matrix elements S_{ij}^I and D_{ij}^I, which are related to the Green's function and its derivative, respectively, inside the cavity are provided elsewhere.[22] In eqs 2 and 3, the first term (i.e., the matrix elements of $\mathbf{S}^I$ and $\mathbf{D}^I$) is independent of the environment, whereas the second and third terms arise from the presence of the SAM−solvent and electrode−SAM interfaces, respectively. In the absence of a SAM, this equation becomes equivalent to the expression derived previously for the electrode−solvent system.[20,22] We have implemented this formulation in the GAMESS electronic structure package[29,30] with technical details analogous to those provided elsewhere.[22]

Figure 2 depicts all of the molecules studied with this IEF-PCM approach. The inner-sphere reorganization energies were calculated using the following expression:[14]

$$\lambda_{in} = \frac{1}{2}[\lambda_{in}^{ox} + \lambda_{in}^{red}]$$
$$= \frac{1}{2}[E_{ox}(R_{eq}^{red}) - E_{ox}(R_{eq}^{ox}) + E_{red}(R_{eq}^{ox}) - E_{red}(R_{eq}^{red})] \tag{4}$$

In this expression, λ_{in}^{ox} and λ_{in}^{red} are the inner-sphere reorganization energies associated with the oxidized and reduced species, respectively, R_{eq}^{ox} and R_{eq}^{red} are the optimized equilibrium geometries of the oxidized and reduced species, respectively, and E_{ox} and E_{red} are the energies of the oxidized and reduced states, respectively, evaluated at the designated geometry. The quantum chemical calculations of the reduced and oxidized species in the gas phase were performed with density functional theory using the B3P86 functional[31,32] with the LANL2DZ[33] basis set for the metal atoms and the 6-31G** basis set for the other atoms using Gaussian 09.[34] The solute reorganization energy was found to be relatively small for this set of transition metal complexes, ranging from 0.02 eV for $[Ru(NH_3)_6]^{3+}$ to 0.15 eV for $[FeCp_2]^+$ for all molecules except TEMPO$^+$, which exhibits a much larger inner-sphere reorganization energy of 0.50 eV. These results reflect the degree of structural change each molecule undergoes upon reduction. The inner-sphere reorganization energies of all of the molecules, as well as results obtained with the M06L functional,[35] are provided in Supporting Information Tables

S2 and S3. Additional tests were performed with the 6-311G** basis set and the B3LYP functional, as given in Supporting Information Table S4. These tests indicate that the results are relatively insensitive to these changes in basis set and functional.

The width of the SAM is calculated in two different ways, depending on whether or not the redox molecule is covalently bonded to the SAM. When the redox molecule is not covalently bonded to the SAM, the sum of the van der Waals radii of the SAM atoms is used to determine the width of the SAM.[36] If the redox molecule is covalently attached to the SAM, an empirically derived formula that also depends on this sum of radii is employed.[28,37] The distance between the center of mass of the molecule and the SAM-solvent interface is chosen to be the radius of a hypothetical sphere with the volume equal to the volume of the molecular cavity generated during the IEF-PCM calculation. All of these distances are given in Supporting Information Table S5.

The calculated total reorganization energies, λ^{PCM}, are compared to the experimental values, λ^{expt}, in Table 1. The

Table 1. Experimental and Calculated Total Reorganization Energies in eV

	λ^{expt}	λ^{PCM}	Δ^a
TEMPO$^+$	1.23−1.53^b	1.43	0.05
$[Ru(NH_3)_6]^{3+}$	0.95^c	0.93	−0.02
$[Ru(NH_3)_5py]^{3+}$	0.88 ± 0.02^d	0.84	−0.04
$[Ru(bpy)_3]^{3+}$	0.56 ± 0.02^d	0.64	0.08
$[FeCp_2]^+$	0.96 ± 0.04^d	0.99	0.03
$[Fe(bpy)_3]^{3+}$	0.56 ± 0.01^e	0.64	0.08
$[Fe(bpy)_2(CN)_2]^+$	0.79 ± 0.02^e	0.72	−0.07
$[Fe(dMbpy)_2(CN)_2]^+$	0.70 ± 0.08^e	0.69	−0.01
$[Fe(bpy)(CN)_4]^-$	0.98 ± 0.04^e	0.84	−0.14
$[Fe(dMbpy)(CN)_4]^-$	0.95 ± 0.06^e	0.83	−0.12
$[Fe(CN)_6]^{3-}$	0.99^f	0.83	−0.16
	1.13 ± 0.02^e		
$[Mo(CN)_8]^{3-}$	0.9^f	0.79	−0.11

$^a\Delta$ is the difference between the value calculated with the IEF-PCM approach and the experimentally measured value. ^{b}Ref 42. ^{c}Ref 36. ^{d}Ref 37. ^{e}Ref 39. ^{f}Ref 38.

total reorganization energies of the positively charged species are reproduced very accurately with this IEF-PCM method, with all deviations less than or equal to 0.08 eV. The breakdown of the total reorganization energy into the inner-sphere and solvent reorganization energies is provided in Supporting Information Table S2. In general, the solvent reorganization energies are much larger in magnitude than the inner-sphere reorganization energies. $[Ru(bpy)_3]^{3+}$ and $[Fe(bpy)_3]^{3+}$ exhibit the smallest solvent reorganization energies (0.6 eV), whereas TEMPO$^+$ exhibits the largest solvent reorganization energy (0.93 eV). The deviations from the experimental results are slightly larger for the negatively charged species, with an apparent systematic error of ca. −0.12 eV. Nevertheless, even these deviations in the reorganization energies are considered acceptable for most applications.

We explored several possible explanations for the larger deviations of the calculated reorganization energies from experimental data for the anionic species. To improve the accuracy of the electronic structure calculations, we performed the inner-sphere and solvent reorganization energy calculations

with larger basis sets including diffuse basis functions, but the results did not change significantly (Supporting Information Table S7). Another possibility is that the errors inherent to DFT are greater for species with excess electronic charge. Furthermore, the molecular cavity for the anionic species could be underestimated, but increasing the size of the molecular cavity decreases rather than increases the solvent reorganization energy.

Another hypothesis is that the negative ions are repelled by the negative potential at the SAM−solvent interface[38] and, thus, are not located directly at this interface. To test this hypothesis, we performed the IEF-PCM calculations at increasing distances d between the molecule and the SAM−solvent interface (Supporting Information Table S8). As expected, we found that increasing this distance by ∼4 Å increases the calculated reorganization energy from 0.85 to 0.90 eV, and increasing this distance by another ∼4 Å increases the reorganization to 0.93 eV, approaching the experimental value of 0.98 ± 0.04 eV. These results suggest that the anions may be located further from the SAM−solvent interface than the cations, leading to slight underestimations of the solvent reorganization energies for the anions. However, this explanation is not consistent with the experimental observation that the rate constants are comparable for anions and cations, or in some cases even larger for anions.[39] On the other hand, these rate constants could also be explained in terms of electron transfer to the cyano groups or desolvation effects.[39]

An alternative explanation is that the ionic strength, which is not included in the model used to obtain the experimental values from the actual experimental data,[38,39] could lead to a systematic deviation. In general, the experimental determination of reorganization energies relies on extrapolation from the measured data and fitting to specific models, thereby leading to substantial differences among various experimental studies.[39] Additional deviations between calculated and experimental values may arise from ion-pairing effects, which have been shown to play a significant role for $[Fe(CN)_6]^{3-}$.[40,41]

We also explored the dependence of the solvent reorganization energy on the width of the SAM. A comparison of the calculated and experimental results for different SAM widths is provided in Supporting Information Table S9. The calculated values are in good agreement with the experimental data, mostly within the reported error bars, and exhibit a relatively small increase in the solvent reorganization energy with the SAM width. We also compared the IEF-PCM results with the three-zone point charge model developed by Liu and Newton.[28] As shown in Supporting Information Table S10, provided that the three-zone point charge model utilizes the same parameters, these two methods generate similar results. In particular, the radius of the molecular sphere, which is also the distance between the molecular center and the SAM−solvent interface, in the three-zone point charge model is chosen to reproduce the volume of the molecular cavity generated by the IEF-PCM method. The agreement between the IEF-PCM results and the analytical three-zone point charge model results indicates that the dominant factors determining the electrochemical solvent reorganization energy are the distance between the molecular center and the SAM−solvent interface, the width of the SAM, and the dielectric constants of the three zones. The IEF-PCM method will be more reliable than the analytical model for molecules that are less spherical and that are characterized by inhomogeneous electron density.

To summarize, we have developed an approach for calculating the solvent reorganization energy for a redox molecule attached to or near a SAM modified electrode. This approach accounts for the effects of the detailed molecular charge redistribution in a molecular-shaped cavity, as well as the electronic and inertial solvent responses and the effects of the SAM and the electrode. The calculated total reorganization energies are in good agreement with experimental data for a series of metal complexes in aqueous solution. This approach will be useful for estimating electron transfer rate constants for electrochemical catalysts and can be further extended to include double layer effects near the electrode for systems without a SAM, as well as the effects due to the ionic strength of the solvent. Moreover, this approach can be expanded to enable the investigation of larger biomolecules that contain redox domains.

■ ASSOCIATED CONTENT

ⓈSupporting Information

Inner-sphere and solvent reorganization energies calculated with B3P86 and M06L functionals; SAM widths and radii associated with molecular cavities; reorganization energies calculated with M06L and B3LYP functionals and larger basis set with diffuse functions; reorganization energies calculated for various SAM widths and for different SAM dielectric constants; comparison of IEF-PCM results with three-zone point charge model results; and coordinates of optimized geometries. This material is available free of charge via the Internet at http://pubs.acs.org.

■ AUTHOR INFORMATION

Corresponding Author
*E-mail: shs3@illinois.edu.

Notes
The authors declare no competing financial interest.

■ ACKNOWLEDGMENTS

■ REFERENCES

(1) Eckermann, A. L.; Feld, D. J.; Shaw, J. A.; Meade, T. J. Electrochemistry of Redox-Active Self-Assembled Monolayers. *Coord. Chem. Rev.* **2010**, *254*, 1769−1802.

(2) Finklea, H. O. Electrochemistry of Organized Monolayers of Thiols and Related Molecules on Electrodes. In *Electroanalytical Chemistry: A Series of Advances*; Bard, A. J., Rubinstein, I., Eds.; Marcel Dekker, Inc.: New York, 1996; Vol. *19*; pp 110−335.

(3) Marcus, R. A. Tight-Binding Approximation for Semi-Infinite Solids. Application of a Transform Method and of Delta Function Normalization. *J. Chem. Phys.* **1993**, *98*, 5604−5611.

(4) Gosavi, S.; Marcus, R. A. Nonadiabatic Electron Transfer at Metal Surfaces. *J. Phys. Chem. B* **2000**, *104*, 2067−2072.

(5) Cave, R. J.; Newton, M. D. CAlculation of Electronic Coupling Matrix Elements for Ground and Excited State Electron Transfer Reactions: Comparison of the Generalized Mulliken−Hush and Block Diagonalization Methods. *J. Chem. Phys.* **1997**, *106*, 9213−9226.

(6) Miller, N. E.; Wander, M. C.; Cave, R. J. A Theoretical Study of the Electronic Coupling Element for Electron Transfer in Water. *J. Phys. Chem. A* **1999**, *103*, 1084−1093.

(7) Matharu, Z.; Bandodkar, A. J.; Gupta, V.; Malhotra, B. D. Fundamentals and Application of Ordered Molecular Assemblies to Affinity Biosensing. *Chem. Soc. Rev.* **2012**, *41*, 1363−1402.

(8) Migliore, A.; Nitzan, A. Irreversibility and Hysteresis in Redox Molecular Conduction Junctions. *J. Am. Chem. Soc.* **2013**, *135*, 9420−9432.

(9) Meredith, M. T.; Minteer, S. D. Biofuel Cells: Enhanced Enzymatic Bioelectrocatalysis. *Annu. Rev. Anal. Chem.* **2012**, *5*, 157−179.

(10) Marcus, R. A. Chemical and Electrochemical Electron-Transfer Theory. *Annu. Rev. Phys. Chem.* **1964**, *15*, 155−196.

(11) Newton, M. D.; Sutin, N. Electron Transfer Reactions in Condensed Phases. *Annu. Rev. Phys. Chem.* **1984**, *35*, 437−480.

(12) Becka, A. M.; Miller, C. J. Electrochemistry at.Omega.-Hydroxy Thiol Coated Electrodes. 4. Comparison of the Double Layer at.Omega.-Hydroxy Thiol and Alkanethiol Monolayer Coated Au Electrodes. *J. Phys. Chem.* **1993**, *97*, 6233−6239.

(13) Marcus, R. A. On the Theory of Electron-Transfer Reactions. VI. Unified Treatment for Homogeneous and Electrode Reactions. *J. Chem. Phys.* **1965**, *43*, 679−701.

(14) Klimkāns, A.; Larsson, S. Reorganization Energies in Benzene, Naphthalene, And Anthracene. *Chem. Phys.* **1994**, *189*, 25−31.

(15) Mikkelsen, K. V.; Pedersen, S. U.; Lund, H.; Swanstroem, P. A New and Rigorous Method for Calculating Intramolecular Reorganization Energies for Electron-Transfer Reactions: Applied for Self-Exchange Reactions Involving Alkyl and Benzyl Radicals. *J. Phys. Chem.* **1991**, *95*, 8892−8899.

(16) Jakobsen, S.; Mikkelsen, K. V.; Pedersen, S. U. Calculations of Intramolecular Reorganization Energies for Electron-Transfer Reactions Involving Organic Systems. *J. Phys. Chem.* **1996**, *100*, 7411−7417.

(17) Cancès, E.; Mennucci, B.; Tomasi, J. A New Integral Equation Formalism for the Polarizable Continuum Model: Theoretical Background and Applications to Isotropic and Anisotropic Dielectrics. *J. Chem. Phys.* **1997**, *107*, 3032−3041.

(18) Cancès, E.; Mennucci, B. New Applications of Integral Equations Methods for Solvation Continuum Models: Ionic Solutions and Liquid Crystals. *J. Math. Chem.* **1998**, *23*, 309−326.

(19) Tomasi, J.; Mennucci, B.; Cammi, R. Quantum Mechanical Continuum Solvation Models. *Chem. Rev.* **2005**, *105*, 2999−3094.

(20) Corni, S.; Tomasi, J. Excitation Energies of a Molecule Close to a Metal Surface. *J. Chem. Phys.* **2002**, *117*, 7266−7278.

(21) Corni, S. The Reorganization Energy of Azurin in Bulk Solution and in the Electrochemical Scanning Tunneling Microscopy Setup. *J. Phys. Chem. B* **2005**, *109*, 3423−3430.

(22) Ghosh, S.; Horvath, S.; Soudackov, A. V.; Hammes-Schiffer, S. Electrochemical Solvent Reorganization Energies in the Framework of the Polarizable Continuum Model. *J. Chem. Theory Comput.* **2014**, *10*, 2091−2102.

(23) Kim, H. J.; Hynes, J. T. Equilibrium and Nonequilibrium Solvation and Solute Electronic Structure. III. Quantum theory. *J. Chem. Phys.* **1992**, *96*, 5088−5110.

(24) Basilevsky, M. V.; Chudinov, G. E.; Napolov, D. V. Calculation of the Rate Constant for the Reaction Chloride + Chloromethane.Fwdarw. $CH_3Cl + Cl^-$ in the Framework of the Continuum Medium Model. *J. Phys. Chem.* **1993**, *97*, 3270−3277.

(25) Mathis, J. R.; Bianco, R.; Hynes, J. T. On the Activation Free Energy of The $Cl^- + CH_3Cl$ SN2 reaction in solution. *J. Mol. Liq.* **1994**, *61*, 81−101.

(26) Cossi, M.; Barone, V. Separation between Fast and Slow Polarizations in Continuum Solvation Models. *J. Phys. Chem. A* **2000**, *104*, 10614−10622.

(27) Miller, C.; Cuendet, P.; Graetzel, M. Adsorbed.Omega.-Hydroxy Thiol Monolayers on Gold Electrodes: Evidence for Electron Tunneling to Redox Species in Solution. *J. Phys. Chem.* **1991**, *95*, 877−886.

(28) Liu, Y.-P.; Newton, M. D. Reorganization Energy for Electron Transfer at Film-Modified Electrode Surfaces: A Dielectric Continuum Model. *J. Phys. Chem.* **1994**, *98*, 7162−7169.

(29) Schmidt, M. W.; Baldridge, K. K.; Boatz, J. A.; Elbert, S. T.; Gordon, M. S.; Jensen, J. H.; Koseki, S.; Matsunaga, N.; Nguyen, K. A.; Su, S.; et al. General Atomic and Molecular Electronic Structure System. *J. Comput. Chem.* **1993**, *14*, 1347−1363.

(30) Gordon, M. S.; Schmidt, M. W. Chapter 41 - Advances in Electronic Structure Theory: GAMESS a Decade Later. In *Theory and Applications of Computational Chemistry*; Dykstra, C. E., Frenking, G., Kim, K. S., Scuseria, G. E., Eds.; Elsevier: Amsterdam, 2005; pp 1167−1189.

(31) Perdew, J. P. Density-Functional Approximation for the Correlation Energy of the Inhomogeneous Electron Gas. *Phys. Rev. B* **1986**, *33*, 8822−8824.

(32) Becke, A. D. Density-Functional Thermochemistry. III. The Role of Exact Exchange. *J. Chem. Phys.* **1993**, *98*, 5648−5652.

(33) Hay, P. J.; Wadt, W. R. Ab Initio Effective Core Potentials for Molecular Calculations. Potentials for K to Au Including the Outermost Core Orbitals. *J. Chem. Phys.* **1985**, *82*, 299−310.

(34) Frisch, M. J.; Trucks, G. W.; Schlegel, H. B.; Scuseria, G. E.; Robb, M. A.; Cheeseman, J. R.; Scalmani, G.; Barone, V.; Mennucci, B.; Petersson, G. A. et al. *Gaussian 09*; Gaussian, Inc.: Wallingford, CT, 2009.

(35) Zhao, Y.; Truhlar, D. G. A New Local Density Functional for Main-Group Thermochemistry, Transition Metal Bonding, Thermochemical Kinetics, and Noncovalent Interactions. *J. Chem. Phys.* **2006**, *125*, -.

(36) Smalley, J. F. Prediction of Standard Interfacial Electron-Transfer Rate Constants for the $Ru(NH_3)_6^{3+/2+}$ Couple through ω-Hydroxyalkanethiol Self-Assembled Monolayers on Gold Electrodes. *J. Phys. Chem. B* **2007**, *111*, 6798−6806.

(37) Smalley, J. F.; Finklea, H. O.; Chidsey, C. E. D.; Linford, M. R.; Creager, S. E.; Ferraris, J. P.; Chalfant, K.; Zawodzinsk, T.; Feldberg, S. W.; Newton, M. D. Heterogeneous Electron-Transfer Kinetics for Ruthenium and Ferrocene Redox Moieties through Alkanethiol Monolayers on Gold. *J. Am. Chem. Soc.* **2003**, *125*, 2004−2013.

(38) Becka, A. M.; Miller, C. J. Electrochemistry at ω-Hydroxy Thiol Coated Electrodes. 3. Voltage Independence of the Electron Tunneling Barrier and Measurements of Redox Kinetics at Large Overpotentials. *J. Phys. Chem.* **1992**, *96*, 2657−2668.

(39) Terrettaz, S.; Becka, A. M.; Traub, M. J.; Fettinger, J. C.; Miller, C. J. ω-Hydroxythiol Monolayers at Au Electrodes. 5. Insulated Electrode Voltammetric Studies of Cyano/Bipyridyl Iron Complexes. *J. Phys. Chem.* **1995**, *99*, 11216−11224.

(40) Khoshtariya, D. E.; Dolidze, T. D.; Zusman, L. D.; Waldeck, D. H. Observation of the Turnover between the Solvent Friction (Overdamped) and Tunneling (Nonadiabatic) Charge-Transfer Mechanisms for a $Au/Fe(CN)_6^{3-/4-}$ Electrode Process and Evidence for a Freezing Out of the Marcus Barrier. *J. Phys. Chem. A* **2001**, *105*, 1818−1829.

(41) Lewis, G. N.; Sargent, L. W. The Potential of the Ferro-Ferricyanide Electrode. *J. Am. Chem. Soc.* **1909**, *31*, 355−363.

(42) Finklea, H. O.; Madhiri, N. Reorganization energies of TEMPO/TEMPO+ in Water. *J. Electroanal. Chem.* **2008**, *621*, 129−133.

5

dx.doi.org/10.1021/jz5023784 | *J. Phys. Chem. Lett.* 2015, 6, 1−5